

# PLZF regulates apoptosis of leukemia cells by regulating AKT/Foxo3a pathway

J.-X. LI<sup>1</sup>, Z.-F. ZHANG<sup>2</sup>, X.-B. WANG<sup>3</sup>, E.-Q. YANG<sup>4</sup>, L. DONG<sup>5</sup>, J. MENG<sup>6</sup>

<sup>1</sup>Department of Clinical Laboratory, Yantaishan Hospital, Yantai, China

<sup>2</sup>Department of Blood Transfusion, Taian City Central Hospital, Taian, China

<sup>3</sup>Department of Clinical Laboratory, The Affiliated Yantai Yuhuangding Hospital of Qingdao University, Yantai, China

<sup>4</sup>Department of Hematology, People's Hospital of Rizhao, Rizhao, China

<sup>5</sup>Department of Hematology, Qianfoshan Hospital Affiliated to Shandong University, Jinan, China

<sup>6</sup>Department of Blood Transfusion, Yankuang New Journey General Hospital, Zoucheng, China

*Jixia Li and Zhifeng Zhang contributed equally to this work*

**Abstract.** – **OBJECTIVE:** To explore the regulatory role of PLZF in the malignant phenotype of non-APL acute myeloid leukemia (AML) and its underlying mechanism.

**MATERIALS AND METHODS:** The expression level of PLZF in AML cell lines KG-1a, HL-60, OCI-AML3, THP-1 and K562 was detected by quantitative Polymerase Chain Reaction (qPCR) and Western blot, respectively. Subsequently, THP-1 cells were divided into mock group (no treatment), scramble group (transfection with scramble shRNA) and shPLZF group (transfection with shPLZF). THP-1 cell line stably expressing shPLZF was constructed, followed by determination of its transfection efficiency by qPCR and Western blot, respectively. The proliferation and colony formation of THP-1 cells were accessed using CCK-8 (cell counting kit-8) assay and colony formation assay, respectively. The apoptotic rate in THP-1 cells was determined using flow cytometry. Protein levels of apoptosis-related genes in THP-1 cells were detected by Western blot. Finally, protein levels of AKT, Foxo3a, pAKT and pFoxo3a were detected by Western blot as well.

**RESULTS:** Both mRNA and protein levels of PLZF were relatively high in THP-1 cells, and were selected for the following experiments. After construction of THP-1 cell line stably expressing shPLZF, proliferative rate and colony formation abilities increased in the shPLZF group compared with the mock group and the scramble group. We found a decreased apoptotic rate, downregulated Bax and upregulated Bcl-2 in the shPLZF group than those of the mock group and scramble group. Phosphorylation levels of AKT and Foxo3a increased after interference with PLZF, whereas no significant changes in total levels of AKT and Foxo3a were observed.

**CONCLUSIONS:** PLZF inhibits the malignant phenotype of AML by regulating the AKT/Foxo3a pathway.

Key Words

PLZF, AML, Proliferation, Apoptosis, AKT.

## Introduction

Since the first case of APL (acute promyelocytic leukemia) with t(11;7)(q23;q21) was discovered in Shanghai<sup>1,2</sup>, 8 cases of this type of APL have been globally reported so far. Chromosomal translocation of the PLZF gene at chromosome 11 and the RAR $\alpha$  gene at chromosome 17 in mouse have been found among the 8 cases<sup>3</sup>. The 7-Kb mRNA transcribed by the PLZF gene encodes a class of zinc finger proteins with transcriptional activity<sup>4</sup>. 118 amino acids in the N-terminal of the PLZF protein encode POZ (poxvirus and Zinc N) or BTB (broad complex, tramtrack, Bric a Brac) domain. The POZ/BTB domain mediates itself or other components, thus forming dimers. It participates in changes of chromosome structure, histone activation and transcriptional repression by interaction with histone deacetylases<sup>5</sup>. There are 9 Kruppel-like C2H2 zinc finger structures at the C-terminal of the PLZF protein, of which KLF1 and KLF2 contain a PML binding function, and KLF3-9 can bind to a specific target gene sequence of PLZF. Two cross-translocation products, PLZF-RAR $\alpha$  and RAR $\alpha$ -PLZF, are generated in APL with t(11;17)(q23;q21)<sup>6,7</sup>. By aberrant activation of the PLZF target gene, RAR $\alpha$ -PLZF is required for malignant transformation or maintenance of APL cells.

Acute myeloid leukemia (AML) is the most common type of leukemia in adults with high heterogeneous. Clinically, some AML cases have reproducible cytogenetic abnormalities, such as characteristics of APL with t(15;17). However, there are still many AML subtypes without specific chromosomal abnormalities<sup>8</sup>. Current studies mostly concentrated on PLZF in APL. Relative researches on PLZF in other AML subtypes are also needed to be carried out. In the present work, we first detected PLZF expression in non-APL-derived myeloid leukemia cell lines and THP-1 cell line was selected for the following experiments. *In vitro* proliferation and apoptosis of THP-1 cells were detected after downregulating PLZF. Our study aims to provide references for developing individualized therapeutic strategies of myeloid leukemia.

## Materials and Methods

### Cells and Reagents

Human myeloid leukemia cell lines HL-60, THP-1 and K562 were purchased from Shanghai Institutes for Biological Sciences (Shanghai, China); OCI-AML3 cell line was gifted from UT MD Anderson Cancer Center. The above myeloid leukemia cells all belonged to non-APL derived AML cell lines.

FBS (fetal bovine serum) was obtained from ExCell Bio (Shanghai, China); Roswell Park Memorial Institute-1640 (RPMI-1640) was obtained from Gibco (Grand Island, NY, USA); Primers were synthesized by Invitrogen (Carlsbad, CA, USA); TRIzol and Real Time-Polymerase Chain Reaction (RT-PCR) kit were purchased from TaKaRa (Otsu, Shiga, Japan); SYBR Premix Ex Taq was purchased from Roche (Basel, Switzerland); RIPA and BCA kit were purchased from Beyotime (Shanghai, China); ECL (electrochemiluminescence), Western Blotting Substrate Kit, and PVDF (polyvinylidene difluoride) membrane were purchased from Merck Millipore (Billerica, MA, USA); PLZF rabbit anti-human polyclonal antibody was obtained from Abcam (Cambridge, MA, USA); Bax rabbit anti-human antibody, Bcl-2 rabbit anti-human antibody, pAKT (S473) rabbit anti-human antibody, pFoxo3a (S253) rabbit anti-human antibody, AKT rabbit anti-human antibody and Foxo3a rabbit anti-human antibody were obtained from Cell Signaling Technology (Danvers, MA, USA);  $\beta$ -actin rabbit anti-human

polyclonal antibody was provided from Proteintech Group (Chicago, IL, USA); IgG goat anti-rabbit was provided from ZSGB Bio (Beijing, China); CCK-8 (cell counting kit-8) reagent kit was provided from Dojindo (Kumamoto, Japan); methylcellulose and puromycin were obtained from Sigma-Aldrich Biotechnology (St. Louis, MO, USA).

### Cell Culture

AML cell lines KG-1a, HL-60, OCI-AML3, THP-1, and K562 were cultured in RPMI-1640 containing 10% FBS, 100 U/mL penicillin and 100  $\mu$ g/mL streptomycin. Cells were maintained in a 5% CO<sub>2</sub> incubator at 37°C.

### Construction of THP-1 Cell Line Stably Expressing shPLZF

PLZF targeting shRNA and shRNA negative control were constructed by Genechem (Shanghai, China). They were sequenced and determined of virus titer. The sequence of PLZF targeting shRNA was 5'-CCCGCAAGACCAACAACAT-3'.

THP-1 cells in logarithmic phase were seeded in the 24-well plate at a density of  $2 \times 10^5$ /mL. According to different treatments, THP-1 cells were divided into mock group (no treatment), scramble group (transfection with scramble shRNA) and shPLZF group (transfection with shPLZF). 100  $\mu$ L of polybrene solution (5  $\mu$ g/mL) containing a proper amount of lentivirus solution was added in each well. Fresh medium was replaced 12 h later. At 72 h, cells were observed for transfection efficacy under a fluorescence microscope. Puromycin was applied at an infectious rate of 80%. Seven days later, THP-1 cell line stably expressing shPLZF was obtained.

### Polymerase Chain Reaction (PCR)

We used TRIzol to extract total RNA for reverse transcription according to the instructions of PrimeScript RT reagent Kit. PLZF band was analyzed by Quantity One software. Furthermore, qPCR was conducted for detecting mRNA level of PLZF. First of all, PLZF primer was constructed according to its sequence published at GeneBank (forward: 5'-AGAGAGGAGTTGAGGGCGAT-3'; reverse: 5'-CCAATAGAGGAGGCGCAGC-3'). The reaction parameters of qPCR were as follows: a total of 39 cycles of pre-denaturation at 94°C for 5 min, denaturation at 94°C for 30 s and annealing at 56°C for 30 s,

followed by extension at 72°C for 10 min. Melting curve condition was set as 65°C-95°C, with temperature elevation at 0.5°C/0.5 s.

### Western Blot

Total protein was extracted by lysate, separated by SDS-PAGE (sodium dodecyl sulphate-polyacrylamide gel electrophoresis) and transferred to PVDF (polyvinylidene difluoride) membranes. Membranes were blocked with 5% skimmed milk, followed by the incubation of specific primary antibodies overnight. Membranes were then incubated with the secondary antibody at room temperature for 1 h. Immunoreactive bands were exposed by enhanced chemiluminescence method and analyzed by Quantity One software.  $\beta$ -actin was used as the loading control.

### CCK-8 Assay

Cells were seeded in 96-well plates with  $2 \times 10^3$  cells per well. Each group set 5 replicates. 10  $\mu$ L of CCK-8 reagent (Dojindo, Kumamoto, Japan) was added in each well at day 0, 1, 2, 3 and 4, respectively. Two hours after the CCK-8 reagent addition, the optical density of each sample was detected at the wavelength of 450 nm using a microplate reader.

### Colony Formation Assay

Cells were resuspended in RPMI-1640 containing 20% FBS. Suspension volume containing 300 cells (V1) and medium volume in each well (V2) were calculated as  $V2 = 750 \mu\text{L} - V1$ . Each group set 3-5 replicates. 750  $\mu$ L of 2.7% methylcellulose was added in each well. After cell culture for 7-14 days, colonies were captured using

an inverted microscope. Colony formation rate = Colonies numbers/Cell number  $\times 100\%$ .

### Flow Cytometry

Cells were seeded in the 6-well plate with  $1 \times 10^6$  cells per well. After incubation for 48 h, cells were collected and centrifuged at 800 r/min for 5 min. Cells were washed with PBS twice and stained with AnnexinV<sup>+</sup>/7-AAD<sup>-</sup> for 15 min in the dark. Apoptotic rate was determined using flow cytometry. Each experiment was performed in triplicate.

### Statistical Analysis

Statistical Product and Service Solutions (SPSS) 17.0 (SPSS Inc., Chicago, IL, USA) and GraphPad Prism 5 (La Jolla, CA, USA) were used for statistical analyses. Data were represented as mean  $\pm$  standard deviation ( $\bar{x} \pm s$ ). One-way ANOVA was used for comparing differences among groups, followed by Post-Hoc Test (Least Significant Difference).  $p < 0.05$  was considered statistically significant.

## Results

### PLZF Expression in AML Cell Lines

PLZF expression in AML cell lines KG-1a, HL-60, OCI-AML3, THP-1 and K562 was detected by qPCR and Western blot, respectively. Both mRNA and protein levels of PLZF were relatively high in THP-1 cells among the detected AML cell lines (Figure 1A and 1B). Hence, THP-1 cells were selected for the following experiments.

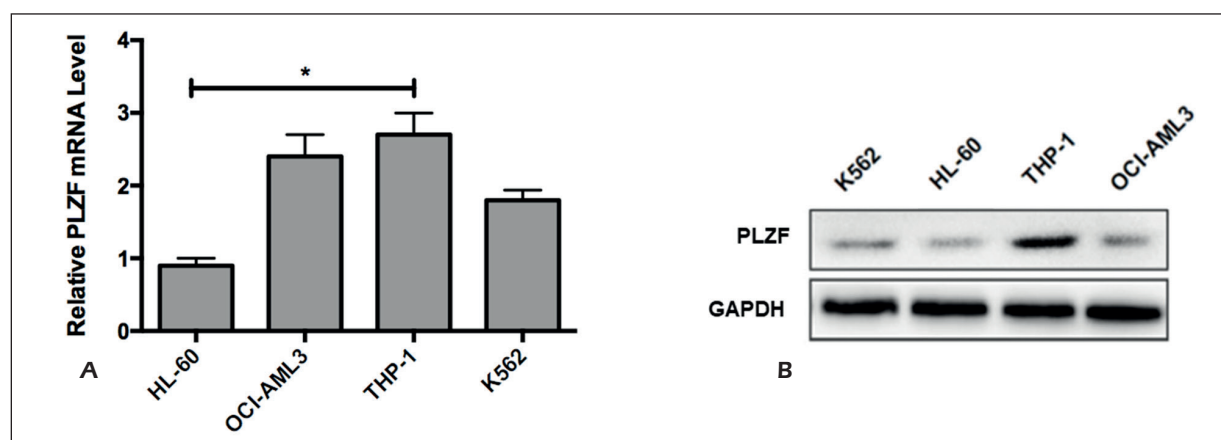


**Figure 1.** PLZF expression in AML cell lines. **A**, The mRNA levels of PLZF in myeloid leukemia cell lines were analyzed by qPCR, and normalized to  $\beta$ -actin. **B**, The protein levels of PLZF in myeloid leukemia cell lines were measured by Western blot and normalized to  $\beta$ -actin. \* $p < 0.05$ .

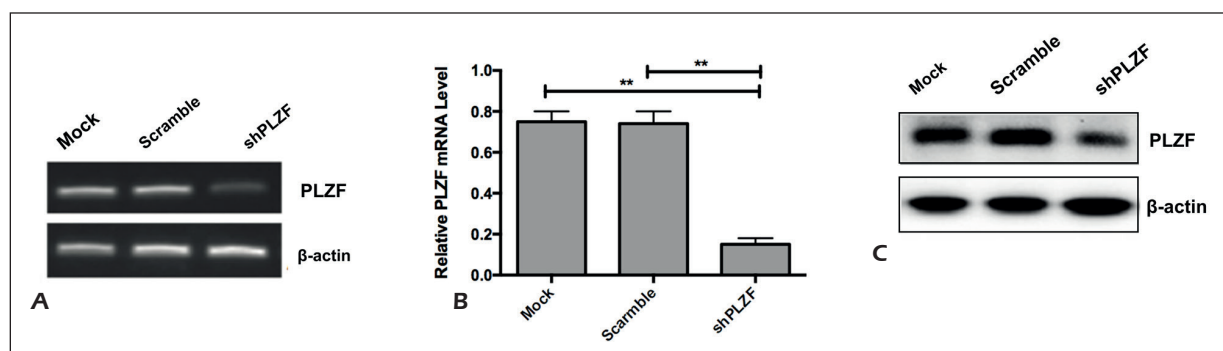


**Figure 2.** Lentiviral-mediated shRNA interfered mRNA and protein levels of PLZF in THP-1 cells. **A**, THP-1 cells were infected with shRNA lentivirus targeting PLZF or its negative control, respectively. RT-PCR was performed to detect PLZF expression and normalized to  $\beta$ -actin. **B**, QPCR was performed to analyze mRNA level of PLZF and normalized to  $\beta$ -actin. **C**, Western blot was performed to measure protein level of PLZF and normalized to  $\beta$ -actin. Mock group: THP-1 cells without treatment; scramble group: THP-1 cells were transfected with shRNA negative control; shPLZF group: THP-1 cells were transfected with shPLZF.  $**p < 0.01$ .

### Lentiviral-Mediated shRNA Interfered mRNA and Protein Levels of PLZF in THP-1 Cells

Based on the different treatments, THP-1 cells were divided into mock group (no treatment), scramble group (transfection with scramble shRNA) and shPLZF group (transfection with shPLZF). Lentiviral-mediated gene knockdown of PLZF was conducted in THP-1 cells of the shPLZF group. QRT-PCR data showed a 200bp PLZF band in the shPLZF group, mock group and scramble group, which was consistent with the expected product size (Figure 2A). The density of PLZF band in the shPLZF group was weaker compared with those of mock group and scramble group. Furthermore, we detected mRNA level of PLZF in THP-1 cells. Lower mRNA level of PLZF was observed in the shPLZF group compared with that of the other two groups ( $p < 0.01$ ). However, no significant change in PLZF level was observed between mock group and scramble group ( $p > 0.05$ , Figure 2B). Similarly, the protein level of PLZF was lower in the shPLZF group than that of the mock group and scramble group as well (Figure 2C). The above data confirmed the successful construction of THP-1 cell line stably expressing shPLZF.

### Effect of PLZF Knockdown on In Vitro Proliferation of THP-1 Cells

CCK-8 assay was conducted to explore the regulatory role of PLZF in the proliferation of THP-1 cells. We found higher proliferative ability of THP-1 cells in the shPLZF group than the mock group and scramble group, especially at day 2 and day 4 ( $p < 0.05$ ). No significant dif-

ference in proliferative rate was found between mock group and scramble group ( $p > 0.05$ , Figure 3). It is suggested that PLZF knockdown could promote *in vitro* proliferation of THP-1 cells.

### Effect of PLZF Knockdown on Colony Formation Ability of THP-1 Cells

To further verify that PLZF could enhance the proliferative capacity of THP-1 cells, colony formation ability of individual cell was observed. Under the inverted microscope, we observed markedly enlarged clones in the shPLZF group (Figure

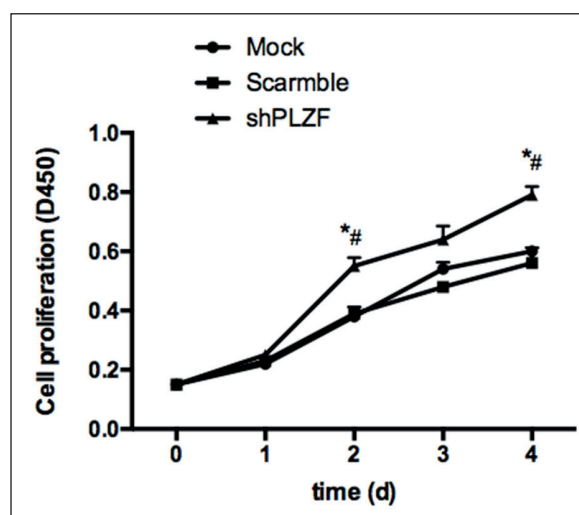
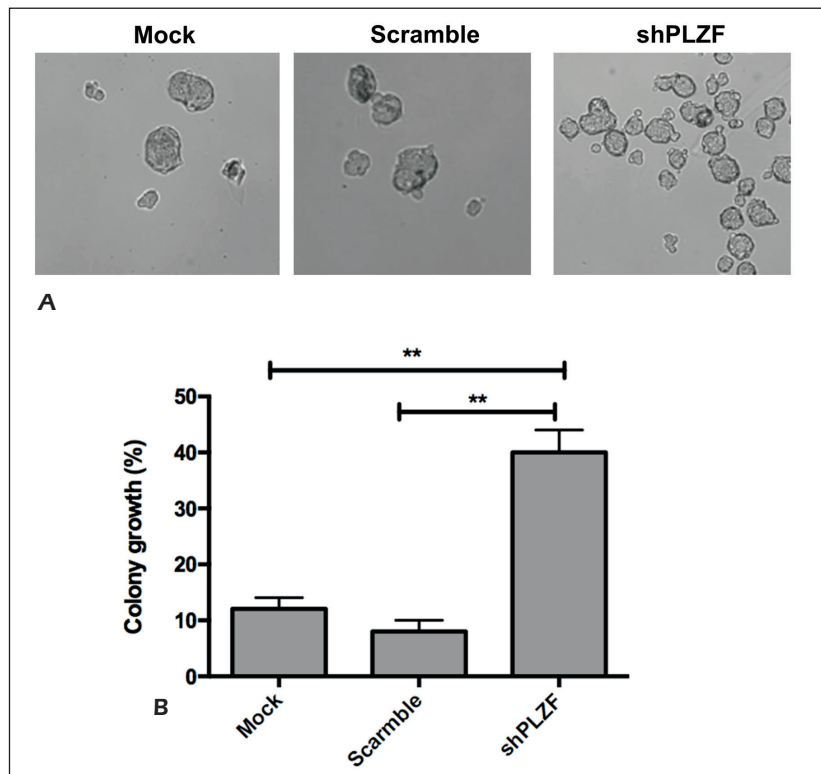


**Figure 3.** Effect of PLZF knockdown on *in vitro* proliferation of THP-1 cells. Proliferative activity of THP-1 cells in mock group, scramble group and shPLZF group was determined by CCK-8 assay.  $*p < 0.05$  compared with mock group;  $#p < 0.05$  compared with scramble group.

**Figure 4.** Effect of PLZF knockdown on colony formation ability of THP-1 cells. **A**, The morphology of cell colonies was observed under microscope (magnification 100×). **B**, Quantification of cell colony rate. \*\* $p < 0.01$ .



4A). Meanwhile, colony formation rate in the shPLZF group ( $18.336\% \pm 0.073\%$ ) was remarkably higher than the mock group ( $6.526\% \pm 0.079\%$ ) and scramble group ( $8.972\% \pm 0.014\%$ ), with a statistical significance ( $p < 0.05$ ). No statistical difference in colony formation rate was found between the mock group and the scramble group ( $p > 0.05$ , Figure 4B).

#### **Effect of PLZF Knockdown on Apoptosis of THP-1 Cells**

The effect of PLZF knockdown on apoptosis of THP-1 cells was determined using flow cytometry. As shown in Figure 5, the apoptotic rate in the shPLZF group ( $18.83\% \pm 1.39\%$ ) was lower than the mock group ( $36.19\% \pm 2.98\%$ ) and the scramble group ( $34.19\% \pm 2.09\%$ ), with a statistical significance ( $p < 0.05$ ). No statistical difference in apoptotic rate was found between the mock group and the scramble group ( $p > 0.05$ ).

Subsequently, Western blot was conducted to determine the protein levels of Bcl-2 and Bax in THP-1 cells. Compared with the mock group and scramble group, upregulated Bcl-2 level and downregulated Bax level were seen in the shPLZF group ( $p < 0.05$ , Figure 6).

#### **Effect of PLZF Knockdown on AKT/Foxo3a Pathway**

To further elucidate the molecular mechanism of PLZF in regulating the proliferation and apoptosis of THP-1 cells, Western blot was performed to detect the expressions of AKT, Foxo3a and their phosphorylation levels in THP-1 cells with PLZF knockdown. Phosphorylation levels of AKT (S473) and Foxo3a (S253) increased after interference with PLZF, whereas no significant changes in total levels of AKT and Foxo3a were observed (Figure 7). We considered that PLZF regulates malignant phenotypes of AML by activating the AKT/Foxo3a pathway.

#### **Discussion**

APL with  $t(11; 17)(q23; q21)$  is susceptible to the formation of the PLZF/RAR $\alpha$  fusion gene. PLZF/RAR $\alpha$  interferes with RAR $\alpha$ /RXR signaling by recruiting co-repressors and HDAC(S) to the RAR $\alpha$  target gene at the BTB/POZ domain, thereby inhibiting the expressions of key factors in granulocyte growth and differentiation<sup>9-12</sup>. In hematological tumors, a fusion gene formed between PLZF and RAR $\alpha$  is the molecular basis

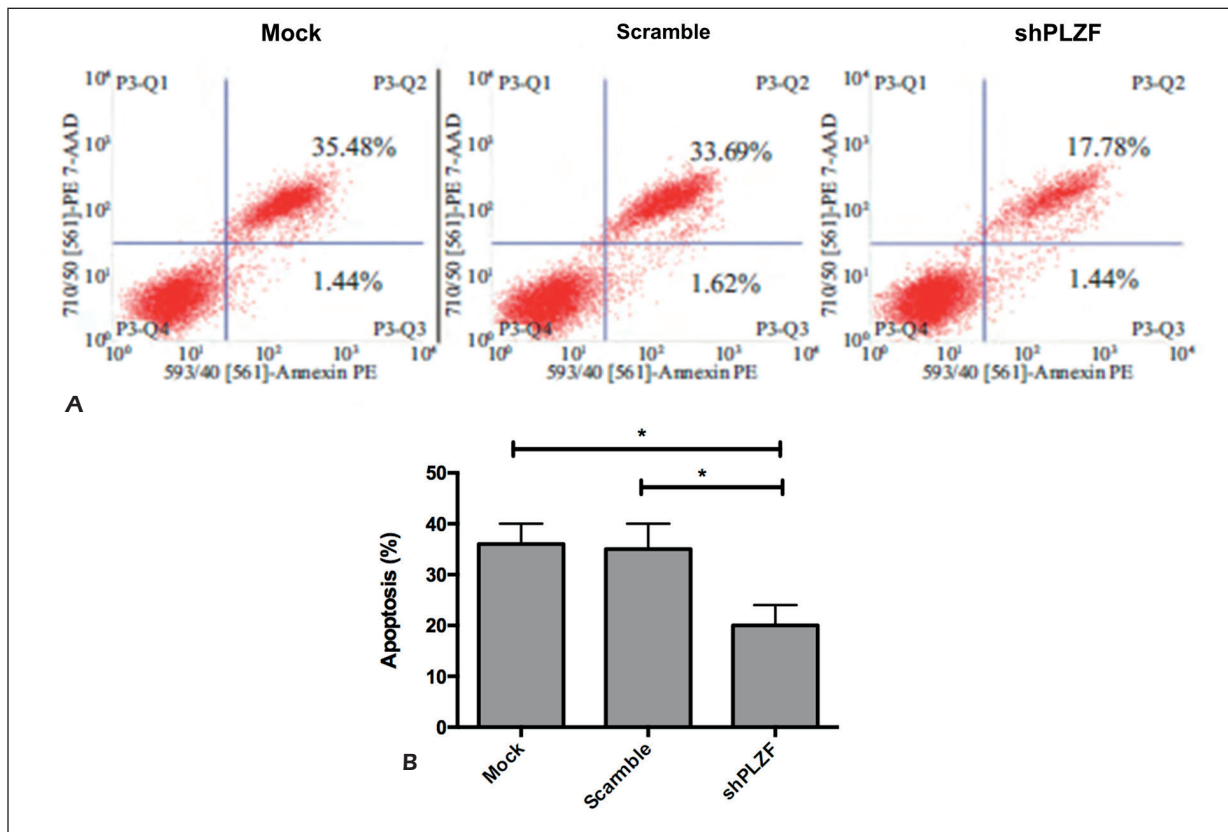


**Figure 5.** Effect of PLZF knockdown on apoptosis of THP-1 cells. **A**, The apoptosis was analyzed by flow cytometry. P3-Q1 represented fragment or damaged cells; P3-Q2 represented percentages of early apoptotic cells; P3-Q2 represented percentages of terminal apoptotic cells; P3-Q4 represented normal cells in mock group. **B**, Apoptotic rate was analyzed by statistics. \* $p < 0.05$ .

for APL occurrence. AML is the most common type of leukemia in adults containing multiple pathological subtypes. We detected the regulatory role of PLZF in the malignant phenotype of non-APL AML. In the present study, we first

detected mRNA and protein levels of PLZF in 5 myeloid leukemia cell lines. Since THP-1 cells expressed a relatively high level of PLZF, they were selected as the experimental object for the subsequent experiments. We next investigated the

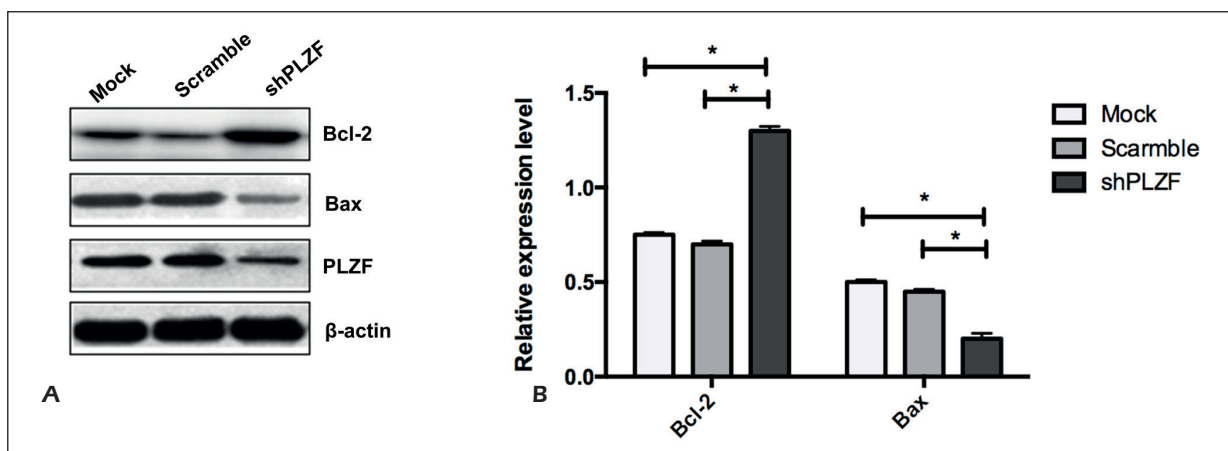


**Figure 6.** Effect of PLZF knockdown on levels of apoptosis-related proteins in THP-1 cells. **A**, Protein levels of apoptosis-related proteins Bcl-2 and Bax were determined by Western blot. **B**, Quantification of protein levels of Bcl-2 and Bax. \* $p < 0.05$ .

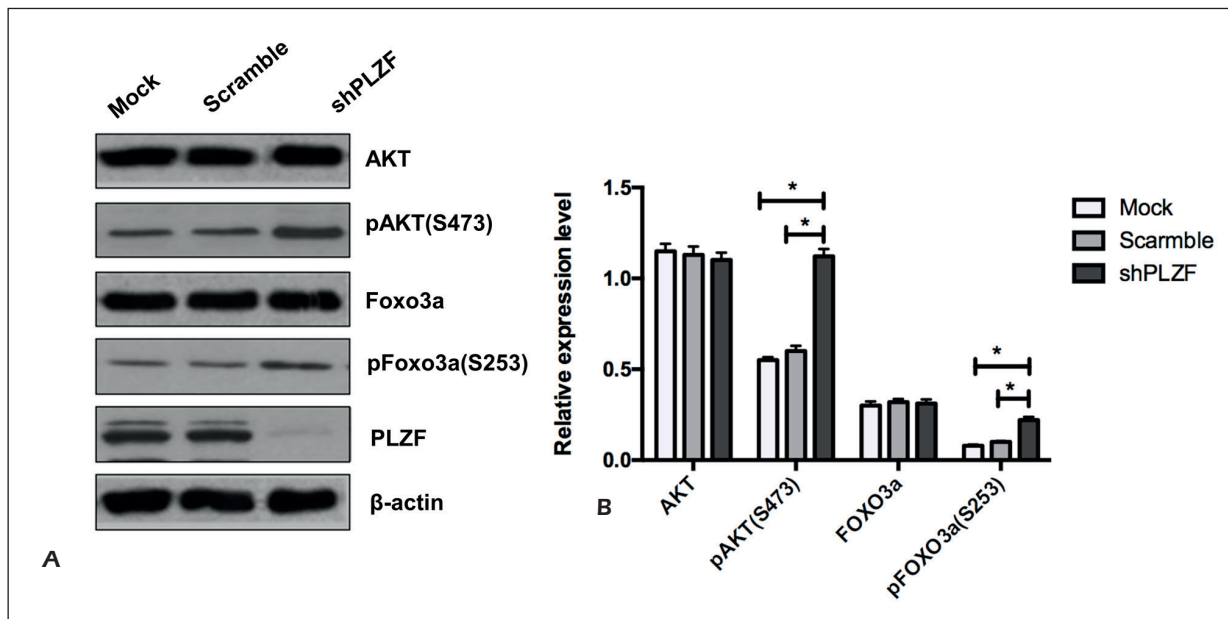


**Figure 7.** Effect of PLZF knockdown on the AKT/Foxo3a pathway. **A**, Protein levels of AKT, Foxo3a, pAKT (S473) and pFoxo3a (S253) were determined by Western blot. **B**, Relative levels of AKT, Foxo3a, pAKT (S473) and pFoxo3a (S253) were quantitatively analyzed. \* $p < 0.05$ .

proliferative and apoptotic capacities of THP-1 cells after downregulation of PLZF. By RNA interference technology, the mRNA and protein levels of PLZF were remarkably downregulated, confirming the THP-1 cell line stably expressing shPLZF was successfully constructed. As a negative regulator of the cell cycle, PLZF could inhibit cell growth by modulating cyclin A2, a necessary factor during the cell cycle transformation from G1 phase to S phase. PLZF downregulates cyclin A2 expression by binding to its promoter, thereby delaying and eventually arresting the cell cycle in S phase. Reversion of cyclin A2 expression abolishes PLZF-induced cell growth inhibition<sup>13</sup>. In this investigation, we found PLZF downregulation enhanced the proliferative rate and decreased the apoptotic rate in THP-1 cells. It is concluded that PLZF exerts an inhibitory effect on the development of myeloid leukemia.

Bcl-2 and Bax are key molecules in the regulation of cell apoptosis. Our results showed that PLZF knockdown remarkably upregulates the anti-apoptotic protein Bcl-2 level and downregulates the pro-apoptotic protein Bax level. The regulation of Bcl-2 and Bax is suggested to be involved in the malignant transformation of THP-1 cells induced by PLZF knockdown. Abnormalities in signal transduction pathways exert a crucial role in the pathogenesis of leukemia. A

persistent activation of AKT has been observed in 50%-80% of AML patients. These patients usually experience lower disease-free survival rate and overall survival compared with those AML patients without AKT activation<sup>14</sup>. As a result, drugs targeting the AKT pathway have been applied in the treatment of AML. As a common downstream gene of AKT, Foxo transcription factor family is capable of inhibiting cell cycle, apoptosis, angiogenesis and migration<sup>15,16</sup>. To investigate whether the AKT/Foxo3a pathway is involved in PLZF-regulated proliferation and apoptosis of THP-1 cells, we first detected the expressions of AKT, Foxo3a and their phosphorylation levels in THP-1 cells with PLZF knockdown. The results showed that the phosphorylation levels of AKT and Foxo3a increased after interference with PLZF. However, no significant changes in total levels of AKT and Foxo3a were observed.

Based on previous literature review and our experimental results, we concluded that PLZF might affect the proliferation and apoptosis of tumor cells by regulating the AKT/Foxo3a pathway. Specifically, PLZF knockdown promoted *in vitro* proliferation but inhibited the apoptosis of AML cells by regulating the AKT/Foxo3a pathway. Further studies are needed to be conducted in clinical samples and experimental animals with AML to elucidate the *in vivo* regulatory role of PLZF.

## Conclusions

We indicated that PLZF knockdown promotes the proliferation and decreases the apoptosis of leukemia cells. We showed that PLZF inhibits the malignant phenotype of AML by regulating the AKT/Foxo3a pathway.

## Funding Acknowledgements

This work was supported by Development Plan of Medical and Health Science and Technology in Shandong Province (2016WS0472); Key R&D Plan in Shandong Province (2018GSF118203).

## Conflict of Interests

The authors declare that they have no conflict of interest.

## References

- 1) CHEN Z, BRAND NJ, CHEN A, CHEN SJ, TONG JH, WANG ZY, WAXMAN S, ZELENT A. Fusion between a novel Kruppel-like zinc finger gene and the retinoic acid receptor-alpha locus due to a variant t(11;17) translocation associated with acute promyelocytic leukaemia. *EMBO J* 1993; 12: 1161-1167.
- 2) CHEN SJ, ZELENT A, TONG JH, YU HQ, WANG ZY, DERRE J, BERGER R, WAXMAN S, CHEN Z. Rearrangements of the retinoic acid receptor alpha and promyelocytic leukemia zinc finger genes resulting from t(11;17)(q23;q21) in a patient with acute promyelocytic leukemia. *J Clin Invest* 1993; 91: 2260-2267.
- 3) SAINTY D, LISO V, CANTU-RAJNOLDI A, HEAD D, MOZZICONACCI MJ, ARNOULET C, BENATTAR L, FENU S, MANCINI M, DUCHAYNE E, MAHON FX, GUTIERREZ N, BIRG F, BIONDI A, GRIMWADE D, LAFAGE-POCHITALOFF M, HAGEMEIJER A, FLANDRIN G. A new morphologic classification system for acute promyelocytic leukemia distinguishes cases with underlying PLZF/RARA gene rearrangements. *Blood* 2000; 96: 1287-1296.
- 4) LICHT JD, SHAKNOVICH R, ENGLISH MA, MELNICK A, LI JY, REDDY JC, DONG S, CHEN SJ, ZELENT A, WAXMAN S. Reduced and altered DNA-binding and transcriptional properties of the PLZF-retinoic acid receptor-alpha chimera generated in t(11;17)-associated acute promyelocytic leukemia. *Oncogene* 1996; 12: 323-336.
- 5) CHANG CC, YE BH, CHAGANTI RS, DALLA-FAVERA R. BCL-6, a POZ/zinc-finger protein, is a sequence-specific transcriptional repressor. *Proc Natl Acad Sci U S A* 1996; 93: 6947-6952.
- 6) HONG SH, DAVID G, WONG CW, DEJEAN A, PRIVALSKY ML. SMRT corepressor interacts with PLZF and with the PML-retinoic acid receptor alpha (RARalpha) and PLZF-RARalpha oncoproteins associated with acute promyelocytic leukemia. *Proc Natl Acad Sci U S A* 1997; 94: 9028-9033.
- 7) SAINTY D, LISO V, CANTU-RAJNOLDI A, HEAD D, MOZZICONACCI MJ, ARNOULET C, BENATTAR L, FENU S, MANCINI M, DUCHAYNE E, MAHON FX, GUTIERREZ N, BIRG F, BIONDI A, GRIMWADE D, LAFAGE-POCHITALOFF M, HAGEMEIJER A, FLANDRIN G. A new morphologic classification system for acute promyelocytic leukemia distinguishes cases with underlying PLZF/RARA gene rearrangements. *Blood* 2000; 96: 1287-1296.
- 8) ZHANG YH, LIN QF, WANG XL, LI QY, CHAI JJ, FAN XJ. Rapamycin induces human acute promyelocytic leukemia cell HL-60 autophagic apoptosis. *Eur Rev Med Pharmacol Sci* 2017; 21: 5506-5514.
- 9) PETTI MC, FAZI F, GENTILE M, DIVERIO D, DE FABRITIS P, DE PROPRIIS MS, FIORINI R, SPIRITI MA, PADULA F, PELICCI PG, NERVI C, LO CF. Complete remission through blast cell differentiation in PLZF/RARalpha-positive acute promyelocytic leukemia: in vitro and in vivo studies. *Blood* 2002; 100: 1065-1067.
- 10) CHOI WI, YOON JH, KIM MY, KOH DI, LICHT JD, KIM K, HUR MW. Promyelocytic leukemia zinc finger-retinoic acid receptor alpha (PLZF-RARalpha), an oncogenic transcriptional repressor of cyclin-dependent kinase inhibitor 1A (p21WAF/CDKN1A) and tumor protein p53 (TP53) genes. *J Biol Chem* 2014; 289: 18641-18656.
- 11) JANSEN JH, LOWENBERG B. Acute promyelocytic leukemia with a PLZF-RARalpha fusion protein. *Semin Hematol* 2001; 38: 37-41.
- 12) RIZZATTI EG, PORTIERES FL, MARTINS SL, REGO EM, ZAGO MA, FALCAO RP. Microgranular and t(11;17)/PLZF-RARalpha variants of acute promyelocytic leukemia also present the flow cytometric pattern of CD13, CD34, and CD15 expression characteristic of PML-RARalpha gene rearrangement. *Am J Hematol* 2004; 76: 44-51.
- 13) YEYATI PL, SHAKNOVICH R, BOTERASHVILI S, LI J, BALL HJ, WAXMAN S, NASON-BURCHENAL K, DMITROVSKY E, ZELENT A, LICHT JD. Leukemia translocation protein PLZF inhibits cell growth and expression of cyclin A. *Oncogene* 1999; 18: 925-934.
- 14) MIN YH, EOM JI, CHEONG JW, MAENG HO, KIM JY, JEUNG HK, LEE ST, LEE MH, HAHN JS, KO YW. Constitutive phosphorylation of Akt/PKB protein in acute myeloid leukemia: its significance as a prognostic variable. *Leukemia* 2003; 17: 995-997.
- 15) DANSEN TB, BURGERING BM. Unravelling the tumor-suppressive functions of FOXO proteins. *Trends Cell Biol* 2008; 18: 421-429.
- 16) GREER EL, BRUNET A. FOXO transcription factors at the interface between longevity and tumor suppression. *Oncogene* 2005; 24: 7410-7425.